Proceedings of GREAT Day

Volume 2020 Article 20

2021

Development of a Time of Flight Spectrometer for Rutherford Backscattering Studies with keV ions

Ethan Smith
SUNY Geneseo

Development of a Time of Flight Spectrometer for Rutherford Backscattering Studies with keV ions

Erratum

Sponsored by Kurt Fletcher

Development of a Time of Flight Spectrometer for Rutherford Backscattering Studies with keV ions

Ethan Smith

sponsored by Kurt Fletcher

Abstract

The solid-state silicon surface barrier (SBD) detectors used in conventional Rutherford backscattering spectroscopy necessitate the use of MeV ion beams, as lower energy ions are stopped in the detectors' dead layer. However, the particle accelerators needed to reach such energies are expensive and often have long startup times. A time of flight spectrometer has been developed at SUNY Geneseo's Low Energy Ion Facility to perform Rutherford backscattering studies using ions with energies in the 10-50 keV range. It has been demonstrated that this spectrometer can accurately measure the kinetic energies of ions scattered off of targets. The spectrometer can also be used to measure the composition and thickness of thin targets. Initial results show good agreement between the results obtained with low energy ions from Geneseo's Duoplasmatron ion source and those obtained via conventional RBS with MeV ions from Geneseo's Pelletron tandem accelerator. Although initial results are encouraging, improvements in resolution and sensitivity must be made before the spectrometer offers the expected advantages.

Rutherford backscattering (RBS) has long been used as a means for characterizing the elemental composition of targets. In Rutherford backscattering experiments, a beam of positively charged ions is incident upon a target sample. The incident ions interact with the nuclei of atoms in the sample via the Coulomb potential and scatter off at an angle, losing some of their energy to the target nucleus. The amount of kinetic energy lost by the incident ion in this collision is characterized by the kinematic factor, k. For an incident ion of mass m scattering off a target nucleus of mass M at an angle θ, the kinematic factor is given by

$$k = \frac{E_f}{E_0} = \left[\frac{(M^2 - m^2\ sin\ sin\ \theta\ )^{\frac{1}{2}} + m\ cos\ cos\ \theta}{M + m}\right]^2$$

Since the kinematic factor is dependent on the mass of the target nucleus, the energy loss of the scattered ion can be used to determine the identity of the target atom. Thus, by measuring the energies of scattered ions, the elemental composition of the target can be determined.

In typical RBS experiments, a beam of high energy particles in the MeV range is directed onto a target, and the energy spectrum of the elastically scattered particles is measured and analyzed. One disadvantage of MeV RBS is that it necessarily requires a particle accelerator able to accelerate ions to those energies. Such particle accelerators are extremely costly and have fairly long start up times. Additionally, beams of such high energy are not as sensitive to trace elements on the surfaces of targets, since a thicker region of the target is sampled by the penetrating ions.

Using lower energy ion beams in the keV range allows for the use of much cheaper and faster ion sources, such as Geneseo's Duoplasmatron ion source at the Low Energy Ion Facility (LEIF). The differential cross section for an ion with energy E and charge Z_1 undergoing Rutherford backscattering off a target nucleus of charge Z_2 at an angle θ is given by

$$\frac{d\sigma}{d\Omega} = \left(\frac{Z_1 Z_2 e^2}{4\pi\epsilon_0 E^2 \left(\frac{\theta}{2}\right)}\right)^2$$

where ϵ_0 is the permittivity of free space and is the charge of the electron. Due to the factor of E^2 in the denominator, lower energy ion beams should offer a higher absolute cross section than high energy beams. In addition, low energy ions have a much shorter range in the target, which makes them more sensitive to trace elements on the surfaces of targets.

However, there are no commercially available detectors able to directly measure the energy spectra of elastically scattered ions in the 20-50 keV range. The standard silicon surface barrier (SSB) detectors used in high energy RBS are not sensitive to ions in this range, as such ions would stop in the dead layer of the SSB detector. Additionally, standard energy detectors are not sensitive to neutral particles.

This paper will discuss the development of a time-of-flight spectrometer based on the design originally laid out by Mendenhall and Weller (1989). The spectrometer will be used for Rutherford backscattering studies using keV ions from a Peabody Scientific Duoplasmatron Ion Source. The start signal will be produced by the scattered ions as they pass through a 5 μg/cm^2 carbon foil, causing it to emit electrons. The secondary electrons are collected by a Channeltron electron multiplier (CEM). The stop signal is

produced by the backscattered ions collected by another CEM at the terminus of the spectrometer. The time between the start and stop detector is the time-of-flight for the ion, which can be used to determine the kinetic energy of the ion.

The Spectrometer

The spectrometer described in this paper was designed as part of the Low Energy Ion Facility (LEIF) at SUNY Geneseo (*Figure 1*). The main component of the LEIF is the PS-120 Peabody Scientific Duoplasmatron ion source. The Duoplasmatron typically produces beams of up to 25 keV deuterons or 50 keV alpha particles, but higher energy beams of heavier ions are possible. The typical beam current output for 50 keV alpha particles is about 20-40 nA, and the ion source can usually be started up in a matter of minutes. The short start up time of the Duoplasmatron confers a distinct advantage over the MeV particle accelerators conventionally used for RBS studies, which can have start-up times on the order of several hours. Used in conjunction with the time-of-flight spectrometer described in this paper, the Duoplasmatron allows for much quicker characterization of surfaces with far less down time.

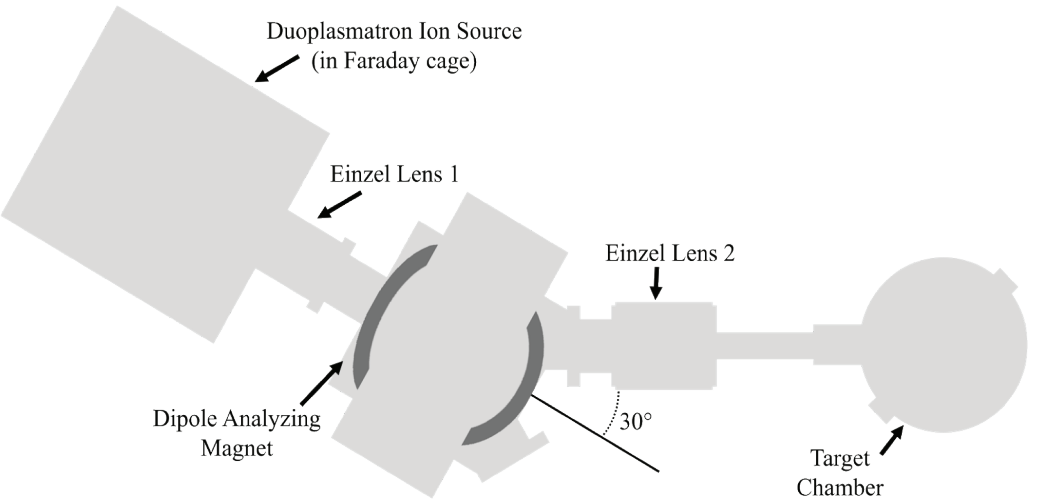

Figure 1: A schematic of the Duoplasmatron ion source at SUNY Geneseo's Low Energy Ion Facility. Ions are extracted from the Duoplasmatron and directed to the target chamber by an analyzing magnet and focused by two einzel lenses along the beam line.

In typical operation, gas is leaked through a needle valve into the Duoplasmatron, where it is ionized into a plasma. The positively charged ions in the plasma are accelerated by an extraction voltage of up to 25 kV. Because the ions exist in multiple charge states inside the plasma, this process allows for the creation of singly charged 25 keV ^{4}He beams or 50 keV beams of doubly charged ^{4}He, for example.

The extracted ions are focused by an electrostatic einzel lens before entering a dipole analyzing magnet, which bends contaminant ion species out of the beam, creating a

high purity monoenergetic beam. In addition, since the entire system is evacuated to pressures on the order of a micro Torr, the ions are able to traverse the entirety of the beam line without significant energy loss. The mean free path for helium ions at these pressures is about 30m.

The ions are then refocused by a second electrostatic einzel lens before being sent through a collimator to the target chamber. The target is held at the center of the scattering chamber by a moveable aluminum arm. The mobility of the target allows for multiple targets to be rotated in and out of the way of the beam without breaking vacuum.

Ions that scatter off the target at an angle of 135° pass through a collimator, entering the time of flight spectrometer arm The scattered ions strike a 5 μg/cm2 (221 Å) carbon foil mounted on a 95% transmission nickel mesh causing the emission of electrons which are accelerated by a voltage of -1500 V toward the start detector. The carbon foil assembly is placed between two grounded nickel grids, so that the path of the incident ion is not significantly altered (*Figure 2*).

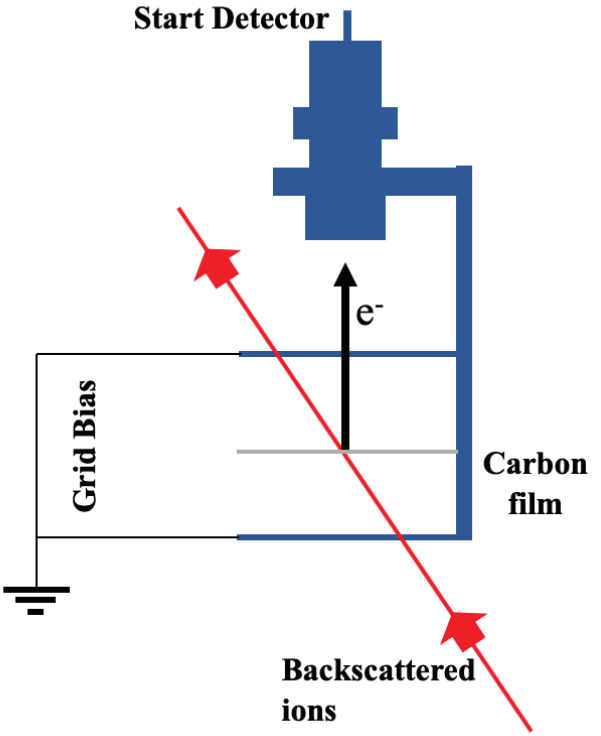

Figure 2: A schematic of the carbon foil assembly used to generate electrons for the start detector. The efficiency of electron production by ions passing through a thin carbon foil is discussed at length (Weller et al., 1994).

There is some energy lost by the scattered ions as they pass through the carbon foil, but this loss can easily be calculated using the free software program Stopping and Range of Ion in Matter (SRIM). For a 50 keV alpha particle scattered off of a gold foil, the energy loss in the carbon foil would be about 4.6 keV or ~10% of the scattered ion's energy. Slower moving ions will tend to lose a greater percentage of their kinetic energy in the foil, and the deviation in that loss will tend to be greater, leading to broader peaks for lighter elements (*Figure 7*).

One drawback of this setup is that ions which undergo charge exchange while passing through the carbon foil will feel a different acceleration between the foil and the second grounded nickel grid than the ion did between the first nickel grid and the foil before the charge exchange took place. This causes some backscattered ions to lose or gain energy in multiples of the foil bias. This effect is presumed to be negligible, as the fraction of ions undergoing charge exchange is small (2014).

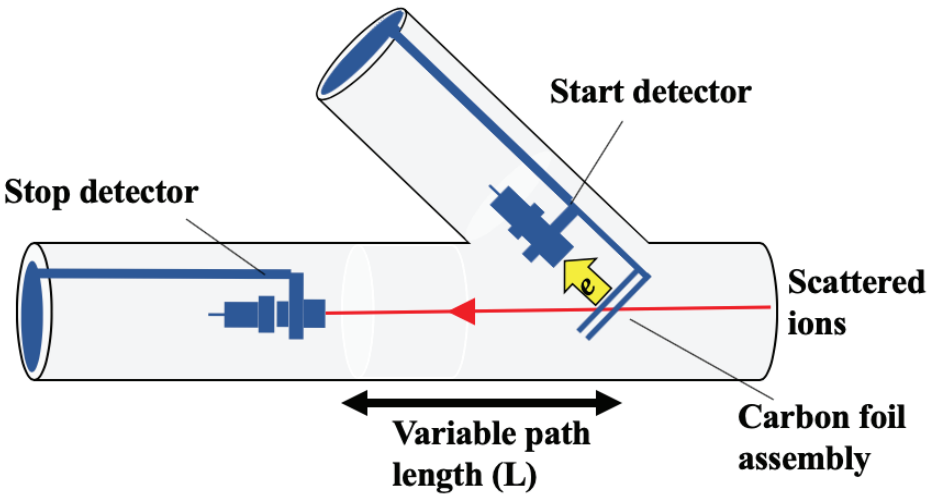

Figure 3: The scattered ions strike the biased carbon foil, causing electrons to be emitted, which are accelerated by a negative bias into the start detector, creating the start signal. The ions continue down the arm of the spectrometer to strike the stop detector.

The scattered ions continue through the carbon foil down a variable path length toward the other CEM, where they produce the stop pulse. Both the start and the stop pulses are fed through an Ortec 579 Fast Filter Amplifier and Ortec 584 Constant Fraction Discriminator to shape the timing pulses before being sent to an Ortec 566 time to amplitude converter (TAC) connected to an Analog Digital Converter (ADC), which collects and bins the signals, producing a time-of-flight spectrum. The time elapsed between when the ADC receives the start and stop pulses is taken to be the time of flight of the particle. Figure 4 shows a typical TAC spectrum for a 50 keV α^{++} beam incident on a 100 Å gold film on a carbon substrate.

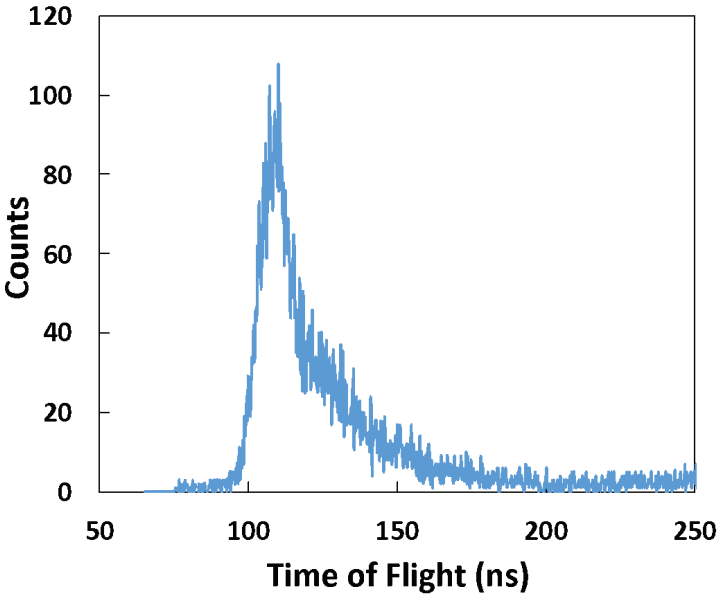

Figure 4: A standard TAC peak for 50 keV α^{++} on a 100 Å gold film on a carbon substrate. The leading edge of the peak represents the time-of-flight of the fastest backscattered ions- i.e. those that scatter directly off the outermost layer of the target.

To verify that the kinetic energies of backscattered ions could be measured using the time-of-flight spectrometer, the path length from the carbon foil to the stop detector was varied, by means of an adjustable, vacuum-tight bellows and the movement of the leading edge of the TAC peak, which represents the time-of-flight of the fastest back-scattered particles, was used to calculate the velocity of the backscattered particles (*Figure 4*).

This process was repeated for thick targets of tantalum and aluminum using both 25 and 50 keV α as well as 25 keV deuterons. Table 1 shows the measured energy values of various ion species on heavy metal targets and theoretical values. The kinetic energy of the ion after scattering off the target nucleus was calculated from kinematics, and the average energy lost by the ions passing through the carbon foil was calculated using the program SRIM.

For example, the kinematic factor for a 50 keV alpha particle scattering off of a 181Ta nucleus at 135° is about 0.927, corresponding to a scattered energy of 46.36 keV. SRIM calculates an average energy of 41.69 keV for an alpha particle of this energy passing through a 221 Å carbon film. The expected deviation in exit energy is ± 0.63 keV or about 1.5%.

Table 1
The kinetic energies measured by tracking the movement of the leading edge show reasonable agreement with theoretical calculations.

Ion Beam	Target	Measured KE (keV)	Predicted KE (keV)
50 keV α^{++}	Gold	43.0 ± 4.4	41.9
50 keV α^{++}	Aluminum	26.3 ± 2.9	26.1
25 keV α^{++}	Tantalum	19.9 ± 1.6	19.7
25 keV d^{+}	Carbon	11.80 ± 0.52	12.23
12.5 keV d^{+}	Tantalum	8.86 ± 0.86	10.36

Analysis

In order to determine the energy of the scattered ions from the measured time of flight, two things must be known: the first is the absolute path length between the carbon foil and the stop detector, and the second is the time of flight of the electrons from the carbon foil to the start detector. The measured time-of-flight, t_m, is related to the actual time of flight of the scattered ion, t_α, by the expression $t_m = t_\alpha - t_e$, where t_e is the transport time of the electron. Therefore, in order to calculate the actual time of flight of the scattered ion, we must add the electron transport time to the nominal time-of-flight read by the TAC.

Based on relativistic kinematics calculations, the maximum kinetic energy imparted to a stationary electron by a head-on collision with a 50 keV α^{++} particle is about 27 eV. Since this is much less than the foil bias, we can assume all emitted electrons start from rest when calculating the transport time for the electrons.

When calculating the time of flight of the electrons, we must consider two regimes: one where the electron is undergoing constant acceleration due to the electric field from the biased foil, and one after it exits the acceleration gap and moves with a constant velocity toward the start detector.

In the acceleration gap, the time of flight of the electron is found using standard constant acceleration kinematics. The emitted electrons feel an electrostatic repulsion that is proportional to the grid bias, and are accelerated across the gap between the carbon foil and the second nickel grid. Thus, the total time for the electron to cross the acceleration gap of length d and bias voltage V is given by

$$t_1 = \sqrt{\frac{2dm_e}{q_e V}}$$

where m_e and q_e are the mass and charge of the electron, respectively.

Given the assumption that the electrons started from rest, the velocity of the electrons after exiting the electric field, v_e is given by

$$v_e = \sqrt{\frac{2q_eV}{d^2m_e}}$$

Thus, the electron drift time t_2 can be calculated by dividing the distance between the second nickel grid and the start detector, l, by the drift velocity. Then the total electron collection time, t_e given by

$$t_e = \sqrt{\frac{2dm_e}{q_eV}} + \sqrt{\frac{l^2d^2m_e}{2q_eV}}$$

A conservative estimate of t_e puts it on the order of 1 ns, which is less than 1% of the typical time of flight of the low energy ions used with this spectrometer. Nevertheless, the collection time should be taken into account when calculating the time-of-flight of the backscattered ions in order to make more accurate measurements.

The spread in electron collection times is likely the main limiting factor on the resolution of this spectrometer (Mendenhall & Weller, 1990). This is a systematic effect that could potentially be corrected for with alternative geometries or bias schemes, but for now the spread is assumed to be negligible on the scale of the large times of flight of the low energy ions used with this spectrometer.

Since the total flight path is difficult to measure directly, the flight path length can be calculated from the intercept of a plot of extension distance versus leading edge time-of-flight. The intercept of the linear fit represents an effective path length from the start detector to the stop detector.

Once the time-of-flight of the scattered ion has been calculated, it must be converted into an energy in order to perform standard RBS analysis. Since the low energies we are dealing with place us squarely in the nonrelativistic regime, the kinetic energy of a scattered ion with mass m and time-of-flight, t, can be calculated by $E=1/2\ m(L/t)^2$, where L is the path length from the carbon foil to the stop detector. Once the energy corresponding to each time-of-flight has been calculated, the time spectrum must be transformed into an energy spectrum by re-binning the data and multiplying by the Jacobian:

$$\left|\frac{dt}{dE}\right| = \frac{t^3}{mL^2}$$

This reshapes the time domain and can amplify any noise in the long-time region of the time-of-flight spectrum due to the factor of t^3 in the numerator. This becomes a problem especially at high beam currents, as the high flux of particles passing through

the spectrometer at these beam currents leads to a higher rate of accidental coincidences especially in the long time-of-flight portion of the spectrum.

Results / Limitations

Time-of-flight spectra for various targets were taken and converted into energy spectra for analysis. These spectra were fit using the simulation software SIMNRA from the Max Planck Institute for Plasma Physics. Figure 5 shows the converted energy spectrum for a 50 keV α^{++} on a 100 Å gold film deposited on a carbon substrate, as well as the fit obtained from SIMNRA. Preliminary results are consistent with results obtained from MeV RBS studies done with Geneseo's 1.7 MV Pelletron tandem accelerator, but at this time the spectrometer does not reach the expected improvements in resolution and sensitivity.

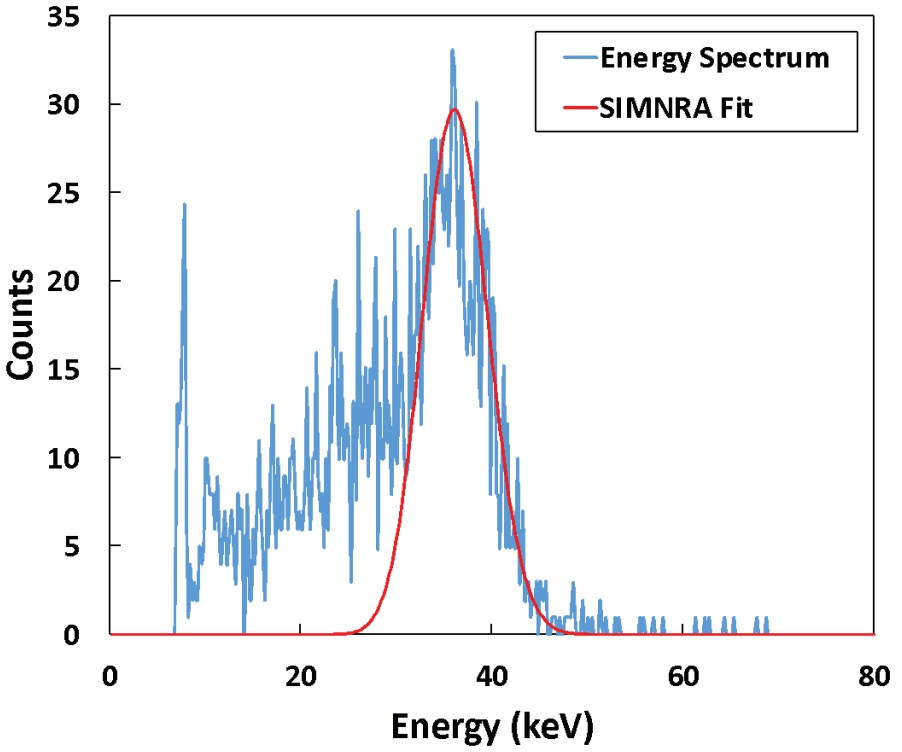

Figure 5: An energy spectrum for a 100 Angstrom gold film deposited on a carbon substrate. Simulation gives a thickness of (103.3 ± 3.1) Å. This agrees with analysis from Geneseo's 1.7 MeV Pelletron linear accelerator, which found a thickness of (101.77 ± 0.71) Å for the same gold target.

One proposed application of the detector described in this work would be for detecting impurities in semiconductors. The increased sensitivity and depth resolution provided by low energy ions should make it easier to detect trace layers of contaminants while providing an accurate measure of a semiconductor's purity. However, the spectrometer was unable to distinguish any difference between a

sample of GaAs doped with carbon, and a sample of GaAs doped with silicon, demonstrating that the spectrometer does not yet possess the resolution and sensitivity necessary for it to be a useful tool.

One reason for this shortfall is that the ion beams used in this study were exclusively isotopes of light ions such as H and He. Due to their low masses, these ions do not offer very good mass resolution for high target masses. Figure 6a shows the kinematic factor for the light deuteron and alpha particle beams, as well as for a heavy ion such as argon. Notice that, for high masses, the curves for d and He beams level off to near constant. Due to this leveling off, it becomes increasingly difficult to distinguish between heavy ions of similar masses. For this reason, the light ion beams used in this study are best suited for lower mass targets, as the difference in kinematic factor is great enough to be detected in that regime.

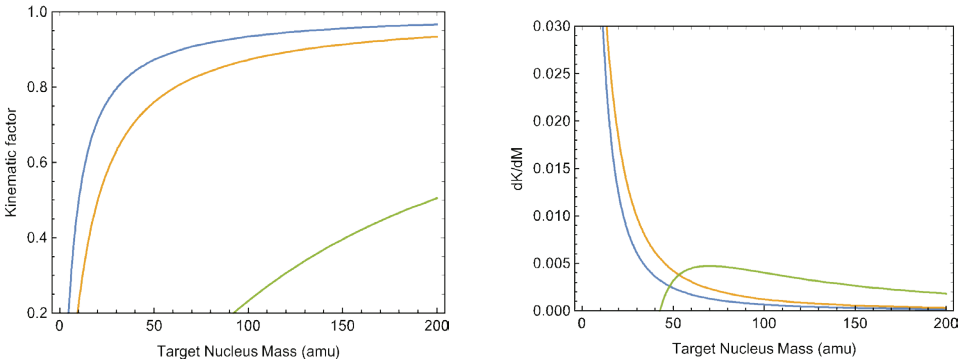

Figure 6: 6a. shows the kinematic factor for d, He, and Ar beams incident on nuclei of various masses. While d and 4He beams have great sensitivity to low mass target nuclei, this is impractical due to physical limitations of the spectrometer, as well as a lower cross section, as dictated by equation (2). 6b. shows the derivative of the kinematic factor with respect to target mass for d, He, and Ar beams. The ion with the greatest value for dk/dM over a particular range has the greatest sensitivity to target nuclei in that range.

However, this poses another problem for the spectrometer, as ions passing through the carbon foil experience a much greater deviation in exit energy, leading to much broader peaks, which further limits the resolution of the detector. Figure 7 shows the effect that this spreading has on the width of the TAC peaks for various elements. In addition, the spectrometer is much less efficient for detecting very low energy scattered particles. Backscattering off of low-Z materials has a much lower differential cross section, making it much more difficult to observe peaks for low-Z elements in the presence of broad, indistinguishable high-Z peaks.

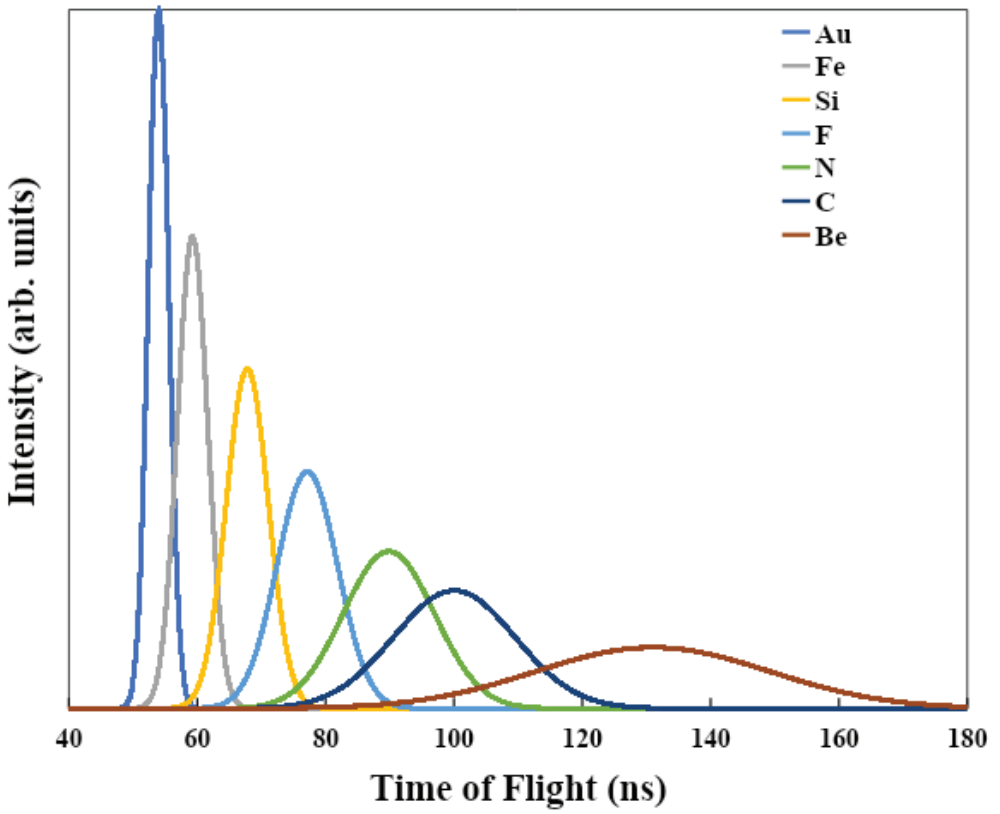

Figure 7: This plot shows the expected spread in measured time of flight for a 50 keV α particle scattering off of various targets before passing through a 5 μg/cm2 carbon foil. This causes time-of-flight peaks for lighter elements to appear more spread out.

At this time, the main issue with the spectrometer is that it is not well-suited for light ions, which are the most easily made and readily available. The easiest solution to this problem would be to switch over to using heavy ion beams such as argon. Heavy ion beams could also potentially allow the Duoplasmatron ion source to operate at energies above the current limit of 50 keV, as heavy ions have a greater number of accessible charge states, allowing them to reach higher kinetic energies when accelerated by a potential difference, as the ions in Geneseo's Duoplasmatron are.

There are, of course, other shortcomings of the spectrometer that need to be addressed in later models. For one, the electron collection method introduces a good deal of uncertainty in the time-of-flight that likely leads to further unnecessary broadening of the peaks. Alternative geometries and bias schemes such as the one described by Mendenhall and Weller (1990) may be able to minimize this effect.

Furthermore, there is the problem that the spectrometer is not well-suited to operate with high beam currents. Due to the nature of the detector, if the beam current is

too high, it tends to overwhelm the system and create far more random coincidences. This can be easily circumvented by applying lower beam currents, but this necessitates longer run times and lower count rates, which worsens the statistics of the spectrum.

Conclusion

The time-of-flight spectrometer described in this work is capable of measuring the energy spectra of ions backscattered off of various targets and does so without the need for an MeV particle accelerator, which are costly in terms of both time and money. However, it is not yet sensitive enough to confer any practical advantage over conventional MeV RBS. While the results obtained to date provide an encouraging proof of concept, limitations on the spectrometer's resolution cast doubt on its future viability. Hopefully, with the requisite improvements the time-of-flight spectrometer can be turned into a powerful tool for surface analysis.

References

Allegrini, F., Ebert, R. W., Fuselier, S. A., Nicolaou, G., Bedworth, P. V., Sinton, S. W., & Trattner, K. J. (2014). Charge state of ~1 to 50 keV ions after passing through graphene and ultrathin carbon foils. *Optical Engineering*, *53*(2), 024101.doi.org/10.1117/1.OE.53.2.024101

Chu, W. K., & Liu, J. R. (1996). Rutherford backscattering spectrometry: reminiscences and progresses. *Materials chemistry and physics*, *46*(2-3), 183-188.

Goebl, D., Bruckner, B., Roth, D., Ahamer, C., & Bauer, P. (2015). Low-energy ion scattering: A quantitative method?. *Nuclear Instruments and Methods in Physics Research Section B: Beam Interactions with Materials and Atoms*, *354*, 3-8. doi.org/10.1016/j.nimb.2014.11.030

Hasegawa, M., Kobayashi, N., & Hayashi, N. (1996). Low-energy Rutherford backscattering-ion channeling measurement system with the use of several tens keV hydrogen and a time-of-flight spectrometer. *Review of scientific instruments*, *67*(10), 3510-3514. doi.org/10.1063/1.1147168

Mendenhall, M. H., & Weller, R. A. (1989). A time-of-flight spectrometer for medium energy ion scattering. *Nuclear Instruments and Methods in Physics Research Section B: Beam Interactions with Materials and Atoms*, *40*, 1239-1243. doi.org/10.1016/0168-583X(89)90628-9

Mendenhall, M. H., & Weller, R. A. (1990). Performance of a time-of-flight spectrometer for thin film analysis by medium energy ion scattering. *Nuclear Instruments and Methods in Physics Research Section B: Beam Interactions with Materials and Atoms*, *47*(2), 193-201. doi.org/10.1016/0168-583X(90)90029-T

Mendenhall, M. H., & Weller, R. A. (1991). High-resolution medium-energy backscattering spectrometry. *Nuclear Instruments and Methods in Physics Research Section B: Beam Interactions with Materials and Atoms*, *59*, 120-123. doi.org/10.1016/0168-583X(91)95189-K

Semrad, D., & Golser, R. (1992). Transformation of time-of-flight spectra into energy spectra for extended targets. *Nuclear Instruments and Methods in Physics Research Section B: Beam Interactions with Materials and Atoms*, *72*(1), 132-138. doi.org/10.1016/0168-583X(92)95292-Y

Weller, R. A. (1993). Instrumental effects on time-of-flight spectra. *Nuclear Instruments and Methods in Physics Research Section B: Beam Interactions with Materials and Atoms*, *79*(1-4), 817-820. doi.org/10.1016/0168-583X(93)95476-L

Weller, R. A., Arps, J. H., Pedersen, D., & Mendenhall, M. H. (1994). A model of the intrinsic efficiency of a time-of-flight spectrometer for keV ions. *Nuclear Instruments and Methods in Physics Research Section A: Accelerators, Spectrometers, Detectors and Associated Equipment*, *353*(1-3), 579-582. doi.org/10.1016/0168-9002(94)91727-2

Zalm, P. C., Bailey, P., Reading, M. A., Rossall, A. K., & van den Berg, J. A. (2016). Quantitative considerations in medium energy ion scattering depth profiling analysis of nanolayers. *Nuclear Instruments and Methods in Physics Research Section B: Beam Interactions with Materials and Atoms*, *387*, 77-85. doi.org/10.1016/j.nimb.2016.10.004